Pathogenic MTOR somatic variant causing focal cortical dysplasia drives hyperexcitability via overactivation of neuronal GluN2C N-methyl-D-aspartate receptors

Louison Pineau, Emmanuelle Buhler, Sarah Tarhini, Sylvian Bauer, Valérie Crepel, Françoise Watrin, Carlos Cardoso, Alfonso Represa, Pierre Szepetowski, Nail Burnashev, et al.

Received: 25 January 2024 | Revised: 19 April 2024 | Accepted: 22 April 2024

DOI: 10.1111/epi.18000

Epilepsia®

RESEARCH ARTICLE

Pathogenic *MTOR* somatic variant causing focal cortical dysplasia drives hyperexcitability via overactivation of neuronal GluN2C N-methyl-D-aspartate receptors

Louison Pineau | Emmanuelle Buhler | Sarah Tarhini | Sylvian Bauer | Valérie Crepel | Françoise Watrin | Carlos Cardoso | Alfonso Represa | Pierre Szepetowski | Nail Burnashev

Institut de Neurobiologie de la Méditerranée, Institut National de la Santé et de la Recherche Médicale, Aix-Marseille University, Marseille, France

Correspondence
Nail Burnashev, Institut de Neurobiologie de la Méditerranée (INMED), INSERM UMR1249, Parc Scientifique de Luminy, BP13, 13273 Marseille Cedex 09, France.
Email: nail.burnashev@inserm.fr

Pierre Szepetowski, Institut de Neurobiologie de la Méditerranée (INMED), INSERM UMR1249, Parc Scientifique de Luminy, BP13, 13273 Marseille Cedex 09, France.
Email: pierre.szepetowski@inserm.fr

Funding information
European Union Seventh Framework Program FP7, Grant/Award Number: 602531

Abstract

Objective: Genetic variations in proteins of the mechanistic target of rapamycin (mTOR) pathway cause a spectrum of neurodevelopmental disorders often associated with brain malformations and with intractable epilepsy. The mTORopathies are characterized by hyperactive mTOR pathway and comprise tuberous sclerosis complex (TSC) and focal cortical dysplasia (FCD) type II. How hyperactive mTOR translates into abnormal neuronal activity and hypersynchronous network remains to be better understood. Previously, the role of upregulated GluN2C-containing glutamate-gated N-methyl-D-aspartate receptors (NMDARs) has been demonstrated for germline defects in the *TSC* genes. Here, we questioned whether this mechanism would expand to other mTORopathies in the different context of a somatic genetic variation of the MTOR protein recurrently found in FCD type II.

Methods: We used a rat model of FCD created by in utero electroporation of neural progenitors of dorsal telencephalon with expression vectors encoding either the wild-type or the pathogenic *MTOR* variant (p.S2215F). In this mosaic configuration, patch-clamp whole-cell recordings of the electroporated, spiny stellate neurons and extracellular recordings of the electroporated areas were performed in neocortical slices. Selective inhibitors were used to target mTOR activity and GluN2C-mediated currents.

Results: Neurons expressing the mutant protein displayed an excessive activation of GluN2C NMDAR-mediated spontaneous excitatory postsynaptic currents. GluN2C-dependent increase in spontaneous spiking activity was detected in the area of electroporated neurons in the mutant condition and was restricted to a critical time window between postnatal days P9 and P20.

Significance: Somatic *MTOR* pathogenic variant recurrently found in FCD type II resulted in overactivation of GluN2C-mediated neuronal NMDARs in

neocortices of rat pups. The related and time-restricted local hyperexcitability was sensitive to subunit GluN2C-specific blockade. Our study suggests that GluN2C-related pathomechanisms might be shared in common by mTOR-related brain disorders.

KEYWORDS
FCD, mTORopathies, neuron, NMDAR

1 | INTRODUCTION

The mechanistic target of rapamycin (mTOR) pathway is an intracellular signaling pathway regulating key cellular processes, including cell growth and metabolism, protein and lipid syntheses, autophagy, and many others via two protein complexes, mTORC1 and mTORC2.[1] In the human brain, excessive, abnormal activation of the mTOR pathway caused by germline or somatic genetic variations results in various epileptic disorders often associated with malformations of cortical development and with behavioral and cognitive impairments.[2–5] Collectively designated as mTORopathies, the related disorders include tuberous sclerosis complex (TSC), hemimegalencephaly, and focal cortical dysplasia (FCD) type II. FCD type II is characterized by cortical dyslamination, neuronal heterotopia, and the presence of dysmorphic neurons (in FCD types IIa and IIb) and of balloon cells (in FCD type IIb only).[6,7] All genetic causes of FCD type II identified so far involve members of the mTOR pathway and lead to hyperactivation of mTORC1; single-hit, gain-of-function pathogenic somatic variants were identified in the eponymous MTOR protein that is part of the mTORC1 complex, or in positive mTOR regulators (e.g., the RHEB protein); also, double-hit loss-of-function defects were reported in negative mTOR regulators (e.g., the TSC proteins hamartin and tuberin, encoded by the *TSC1* and *TSC2* genes, respectively; the GATOR1 complex proteins DEPDC5, NPRL2, and NPRL3). Altogether, genetic variants of the mTOR pathway have been identified in 30%–60% of type II FCDs.[8,9]

Upregulation of the mTOR pathway is an important cause of severe epilepsy; mTORopathies are the most common cause for intractable epilepsy in childhood.[5] Overall, FCDs represent the most frequent cause of drug-resistant focal epilepsy in children.[10] FCD type II represents the most frequent subtype of all FCDs. However, pharmacological and surgical management of the patients remains unsatisfactory. Hence, identification of the pathomechanisms associated with variations of the mTOR pathway is needed. Although several cell-autonomous and non-cell-autonomous mechanisms have been proposed in various rodent models,[5,11,12] how the numerous genetic variants in different members of the mTOR pathway lead to abnormal neuronal activity and to a hypersynchronous network remains to be clarified.

Key points

- Excessive activation of GluN2C NMDAR-mediated currents was seen in spiny stellate neurons expressing FCD-causing MTOR somatic variation.
- GluN2C-dependent increase in spontaneous spiking activity was seen in rat somatosensory cortex containing mutant MTOR-expressing neurons.
- GluN2C-dependent local hyperexcitability is time-restricted to a critical period between P9 and P20.

Glutamate-gated N-methyl-D-aspartate (NMDA) receptors (NMDARs) are instrumental to synchronicity of neuronal networks, and NMDARs dysfunction is associated with a broad spectrum of developmental brain disorders, including epilepsy. NMDARs are di- or triheterotetramers composed of two obligatory GluN1 and two GluN2(A-D)/GluN3(A,B) subunits. Much of the functional difference between NMDARs subtypes is attributed to GluN2/3 subunit identity. GluN2/GluN3 subunits show different temporal and spatial expression patterns in the brain; furthermore, NMDAR composition vary depending on cell types and subcellular localization.[13] Previously, we showed that neuronal currents mediated by GluN2C-containing NMDARs in the neocortex played a major epileptogenic role in $Tsc^{+/-}$ mice and in surgically removed tissue not only from TSC patients, but also from genetically uncharacterized FCD patients.[14] Slower deactivation kinetics of GluN2C-containing NMDARs would sustain increased synaptic integration and hypersynchrony of neuronal networks. Whether this appealing GluN2C-mediated pathogenic mechanism associated with *TSC1*/*TSC2*

defects is expandable to other members of the mTOR pathway and to their related disorders, and whether it would be operating in the mosaic context of the somatic variations seen in type II FCDs, are important and related questions that have not been addressed yet.

We designed a rat model of FCD type II where a pathogenic, recurrent somatic variant (p.S2215F) of the MTOR protein was expressed in a subset of neuronal excitatory cells of the somatosensory cortex by in utero electroporation of the appropriate expression vector in neural progenitors of the dorsal telencephalon.[15] In this model, the affected focal area is composed by electroporated neurons (expressing the mutant MTOR protein) and by nonelectroporated (nonmutant) cells. This situation mimics the cellular mosaicism seen in FCD type II, where MTOR-p.S2215F or other somatic variations in genes of the mTOR pathway arise in a subset of neuronal cells, then expressing the mutant isoform of the corresponding protein in the brain malformation, whereas other cells express only the wild-type (WT) isoform. In line with previous reports indicating that the recurrent MTOR-p.S2215F variation leads to increased MTOR kinase activity,[16–18] electroporated cells showed increased S6 phosphorylation consistent with mTORC1 overactivation as well as abnormal migration and dysmorphology.[15] Here, the functional effects of the pathogenic MTOR-p.S2215F variation on neuronal NMDARs and local network activities, and the possible involvement of GluN2C-mediated NMDAR currents in pathogenesis, were analyzed in the mosaic context of this rat model of mTOR-related FCD type II.

2 | MATERIALS AND METHODS

More detailed information on the experimental procedures and analyses are provided as Supplementary Material and Methods.

2.1 | In utero electroporation

Wistar rats (Janvier Labs) were raised and mated at the INMED animal facility (controlled temperature at 21–23°C, food and water ad libitum, 12–12-h dark–light cycle). In utero intracerebroventricular injections and electroporations of the embryonic brains with either WT or mutant MTOR expression vectors (pCAG-MTOR WT-IRES-GFP or pCAG-MTOR-p.S2215F-IRES-GFP, respectively; 3.0 μg/μL each) or nonrecombinant pCAGIG-GFP vector (pCAG-IRES-GFP; .5 μg/μL) were performed from timed pregnant rats at embryonic day 15.5 (E15.5) as previously described,[15] except that isoflurane (4% for induction, then 2.5%) was used instead of sevoflurane.

2.2 | Single-cell patch-clamp recordings and analyses

Coronal neocortical slices (300 μm thick) were obtained from postnatal day 9 (P9) and P14–P16 pups and preincubated as previously done.[14] Whole-cell patch-clamp recordings in somatosensory cortex of electroporated (green fluorescent protein [GFP]$^+$) and their adjacent (<20 μm distance) nonelectroporated (GFP$^-$) cells that displayed typical electrophysiological and morphological properties of spiny stellate neurons (SSNs), which represent the majority (58%–77%) of all excitatory neurons in layer 4 of somatosensory cortex in rodents,[19,20] were performed at room temperature (22–25°C) in Mg^{2+}-free medium to obtain the contribution of the NMDAR-mediated component. Neuronal action potential (AP) firing pattern and intrinsic properties were recorded in current-clamp configuration. spontaneous excitatory postsynaptic currents (sEPSCs) were recorded in voltage clamp mode at −75 mV (reversal potential of γ-aminobutyric acidergic [GABAergic] currents) without or with the following NMDAR blockers: 10 μmol·L^{-1} DQP 1105 (Tocris Bio-Techne), 10 μmol·L^{-1} DQP 1105 + 1 μmol·L^{-1} Ro 25–6981 (Tocris Bio-Techne), 50 μmol·L^{-1} APV (2-amino-5-phosphonovaleric acid, Hello Bio). Rapamycin-based experiments were performed with daily intraperitoneal injections during seven consecutive days (P8–P14) prior to the P14–P16 recordings of either rapamycin or only the vehicle, as described previously.[14] sEPSCs were analyzed using MiniAnalysis 6.0.3 software (Synaptosoft), and averaged traces were analyzed with Origin software (MicroCal). In some experiments, spontaneous APs were recorded in current-clamp mode, detected based on AP waveforms, and numbers of AP were plotted versus selected time intervals for comparison between conditions.

2.3 | Extracellular recordings and analyses

Slices were obtained from P9, P14–P16, and P20–P21 pups as above. Recordings were done in the electroporated area at room temperature (22–25°C) in oxygenated Mg^{2+}-containing medium using a coated nichrome electrode. Spontaneous activity was recorded without or with NMDAR blockers DQP 1105 or APV (see above). Files were analyzed using Clampfit (Molecular Devices). Rapamycin injections were as above.

2.4 | Electroencephalographic recordings

Cortical electroencephalography (EEG) was performed on postnatal days P60–P70 in freely moving MTOR-p.S2215F and MTOR-WT electroporated rats and analyzed as done previously.[21]

2.5 | Immunohistochemistry

Brains slices from P15 pups were processed for Rorβ and GFP immunostaining as detailed in Supplementary Material and Methods.

2.6 | Histological reconstruction of neurons

A subset of whole-cell recorded neurons was filled with biocytin before the sections were processed for imaging using confocal microscopy and neuronal reconstruction with Neurolucida software, as reported previously.[14]

2.7 | Statistics

Comparison of groups was done with Mann–Whitney test (datasets = 2) or with Kruskal–Wallis test followed by Dunn's correction for multiple testing (data sets > 2). Friedman test with Dunn's post hoc correction was used to analyze the effect of DQP 1105 and APV on the frequency of APs in MTOR-p.S2215F extracellular recordings. Effects of drugs on sEPSC area was analyzed with a mixed-effect model followed by Tukey multiple comparison test. For all comparisons, sex ratio did not differ significantly between conditions (Fisher exact test). All values are given as mean ± SD. Level of significance was set at $p < .05$. Raw data are provided as Tables S1–S9.

3 | RESULTS

3.1 | Mutant MTOR-p.S2215F neurons display decreased cell input resistance and increased capacitance

We used a previously characterized model of FCD[15] created by in utero electroporation of vectors for the coexpression of GFP with either of the mutant MTOR-p.S2215F or the WT MTOR isoforms in neural progenitors from the somatosensory cortex of rat embryos at E15.5. This model was characterized by neuronal dyslamination; in line with the neuronal migration defects that had been observed with the mutant but not with the WT isoform in prenatal brains at E20, MTOR-p.S2215F electroporated neurons were not detected in layer 4 of the somatosensory cortex and remained located in deeper cortical layers and in corpus callosum at P15 (Figure S1). This model was also characterized by epileptic activity, as assessed by telemetric EEG in rats aged P60–P70 (Figure S2, Table S1) and as also reported in the corresponding mouse model.[22] We first studied the activity of neurons expressing MTOR-p.S2215F compared to neurons expressing MTOR-WT using patch-clamp recordings in brain slices from P14–P16 rats previously electroporated in utero. This developmental period corresponded to the critical time window when GluN2C-containing NMDARs played a major epileptogenic role in $Tsc^{+/-}$ mice.[14] We also electroporated the construct that encodes GFP (GFP-only) as a control. Recordings from SSNs, in which overexpressed GluN2C-mediated currents were detected in TSC,[14] were selected based on their distinct firing properties compared to pyramidal cells. Analysis of the firing pattern elicited by depolarizing steps revealed that MTOR-p.S2215F neurons displayed significantly decreased input resistance (Rinput) and increased capacitance (Cm) compared to MTOR-WT and GFP-only neurons (MTOR-p.S2215F: Rinput = 241.3 ± 69.98 MΩ, Cm = 246.2 ± 106.2 pF; MTOR-WT: Rinput = 529.5 ± 276.3 MΩ, Cm = 80.1 ± 46.67 pF; GFP: Rinput = 413.9 ± 120 MΩ, Cm = 75.16 ± 20.83 pF), whereas no significant difference was detected between MTOR-WT and GFP-only neurons (MTOR-p.S2215F vs. MTOR-WT: pRinput = .0006 and pCm < .0001; MTOR-p.S2215F vs. GFP: pRinput = .0169 and pCm < .0001; MTOR-WT vs. GFP: pRinput > .9999 and pCm = .8842; Figure 1, Table S2). Consistent with the altered input resistance and capacitance in MTOR-p.S2215F neurons, and with their previously reported increased cell size,[15] post hoc reconstruction of biocytin-filled recorded cells at P14–P16 revealed significant increase of the soma volume and dendrite surface area of MTOR-p.S2215F neurons compared to MTOR-WT neurons (Figure S3, Table S3). No significant change in other neuronal intrinsic properties was detected (Figure S4, Table S2). Nonelectroporated GFP^- neurons adjacent to electroporated GFP^+ mutant MTOR-p.S2215F neurons displayed unaltered input resistance and membrane capacitance, as for MTOR-WT neurons (Figure S5, Table S4).

3.2 | Upregulation of NMDAR-mediated currents in mutant MTOR-p.S2215F neurons

Next, we analyzed sEPSCs at −75 mV in Mg^{2+}-free artificial cerebrospinal fluid to access the contribution of α-amino-3-hydroxy-5-methyl-4-isoxazolepropionic acid (AMPA)

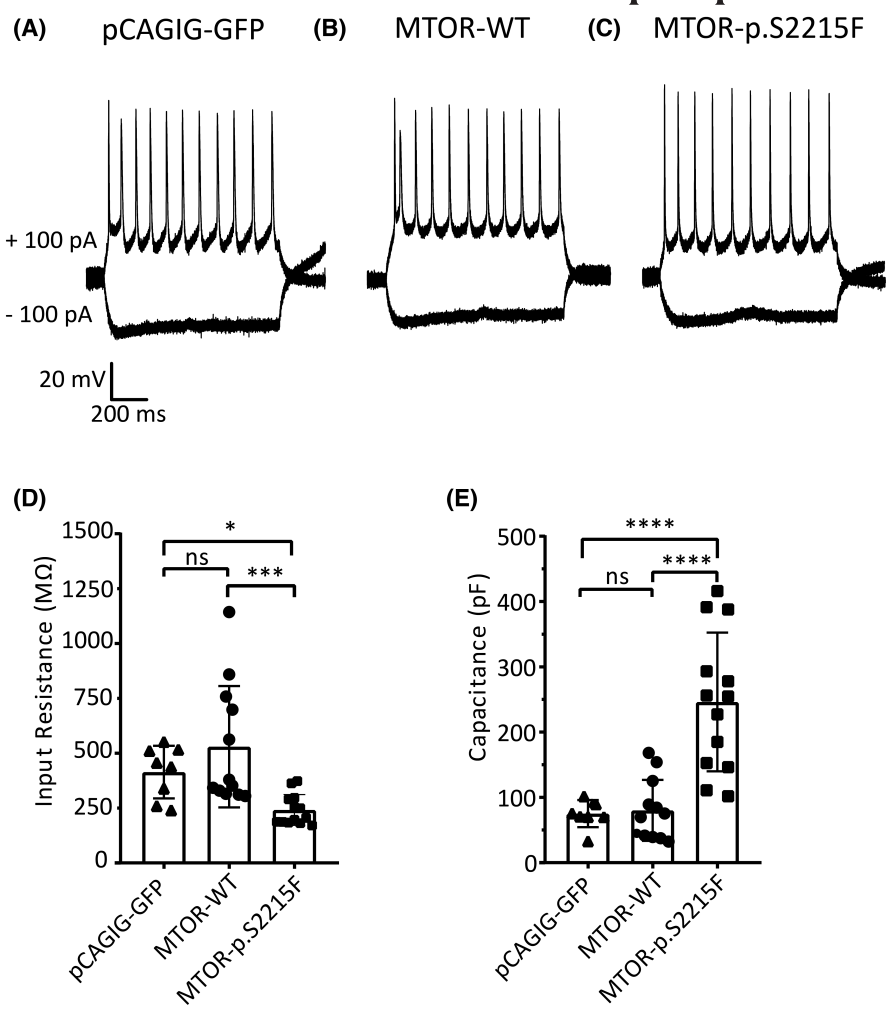

FIGURE 1 Action potential firing pattern and membrane properties of electroporated neurons. Example traces are shown of action potential firing patterns of spiny stellate neurons recorded in current-clamp mode upon depolarizing and hyperpolarizing current injections into the cells and expressing either of the following: (A) green fluorescent protein (GFP) only (pCAGIG-GFP), (B) mechanistic target of rapamycin–wild type (MTOR-WT), and (C) mutant MTOR-p.S2215F. (D) Neuronal input resistance and (E) capacitance values in GFP-only ($n = 8$ neurons from seven pups), MTOR-WT ($n = 12$ neurons from 11 pups), and mutant MTOR-p.S2215F ($n = 13$ neurons from 11 pups) conditions. *$p < .05$, ***$p < .001$, ****$p < .0001$; ns, not significant; Kruskall–Wallis test followed by Dunn post hoc test.

receptors (AMPARs) and NMDAR-mediated currents to the total sEPSCs. Mutant MTOR-p.S2215F neurons looked more active than MTOR-WT neurons (Figure 2A), and analysis of the normalized-to-the-peak averaged sEPSCs revealed an increased contribution of the slow component to the total sEPSCs (Figure 2B), most likely indicating elevation of the NMDAR-mediated currents with slow decay kinetics, reflected as increased charge transfer in the mutant condition (Figure 2C, Table S5). Importantly, sEPSCs from the nonelectroporated GFP^- neurons adjacent to electroporated GFP^+ mutant MTOR-p.S2215F neurons were not different from MTOR-WT neurons and from GFP-only neurons (Figure S6). The increased contribution of NMDARs in mutant cells was confirmed in experiments with APV, a selective blocker of total NMDAR-mediated currents. Although no change in the amplitude of AMPAR-mediated component of the total sEPSC in the presence of APV was observed (Figure 2D,E), the ratio of the NMDA/AMPA amplitudes significantly increased from $.3412 \pm .2751$ in MTOR-WT neurons to $1.635 \pm .5749$ in mutant MTOR-p.S2215F neurons ($p = .0006$; Figure 2F, Table S6).

To discriminate between the respective contributions of different NMDAR subunits in increased NMDAR-mediated currents with slow decay kinetics in the total sEPSCs, we used the following subunit-selective NMDAR blockers: DQP 1105 for GluN2C/D-mediated component and Ro 25-6981 for GluN2B-mediated component. Comparison of the averaged sEPSC areas revealed that DQP 1105 significantly reduced the total sEPSC area whereas Ro 25-6981 did not have any significant additional effect (no drug vs. DQP: $p = .0054$; DQP vs. DQP+Ro: $p = .1221$; Figure 3, Table S7). As a possible contribution of GluN2D in the recorded sEPSCs was excluded based on the decay kinetics of the component inhibited by DQP 1105, these results suggested a major contribution of GluN2C-mediated currents to increased NMDAR-mediated component of the total sEPSCs. Also, as expected, administration of the mTOR inhibitor rapamycin to the pups prior to the patch-clamp recordings restored proper neuronal input resistance and membrane capacitance (Figure 4A–C), and led to decreased contribution and faster decay kinetics of NMDAR-mediated currents in mutant neurons (Figure 4D–F, Table S5); consistent with the lack of GluN2C-mediated effects in this rescue condition,

DQP 1105 did not have any significant impact on total sEPSC (Figure S7, Table S7).

3.3 | MTOR-p.S2215F variation causes increased spontaneous and time-restricted spiking activity driven by NMDAR-GluN2C currents

Increased sEPSC area associated with increased contribution of the GluN2C-mediated component with the slow decay kinetics indicated an increased integration time window for excitatory inputs, providing increased spiking activity of the mutant neurons. Current-clamp experiments showed an increased and longer lasting spiking activity in mutant cells that was reduced upon DQP 1105 application (Figure S8). We thus decided to more precisely address the impact of increased GluN2C-mediated neuronal currents on local network activity. To this aim, we studied the spontaneous spiking activity of the electroporated area using extracellular recordings in coronal slices from rat pups at ages

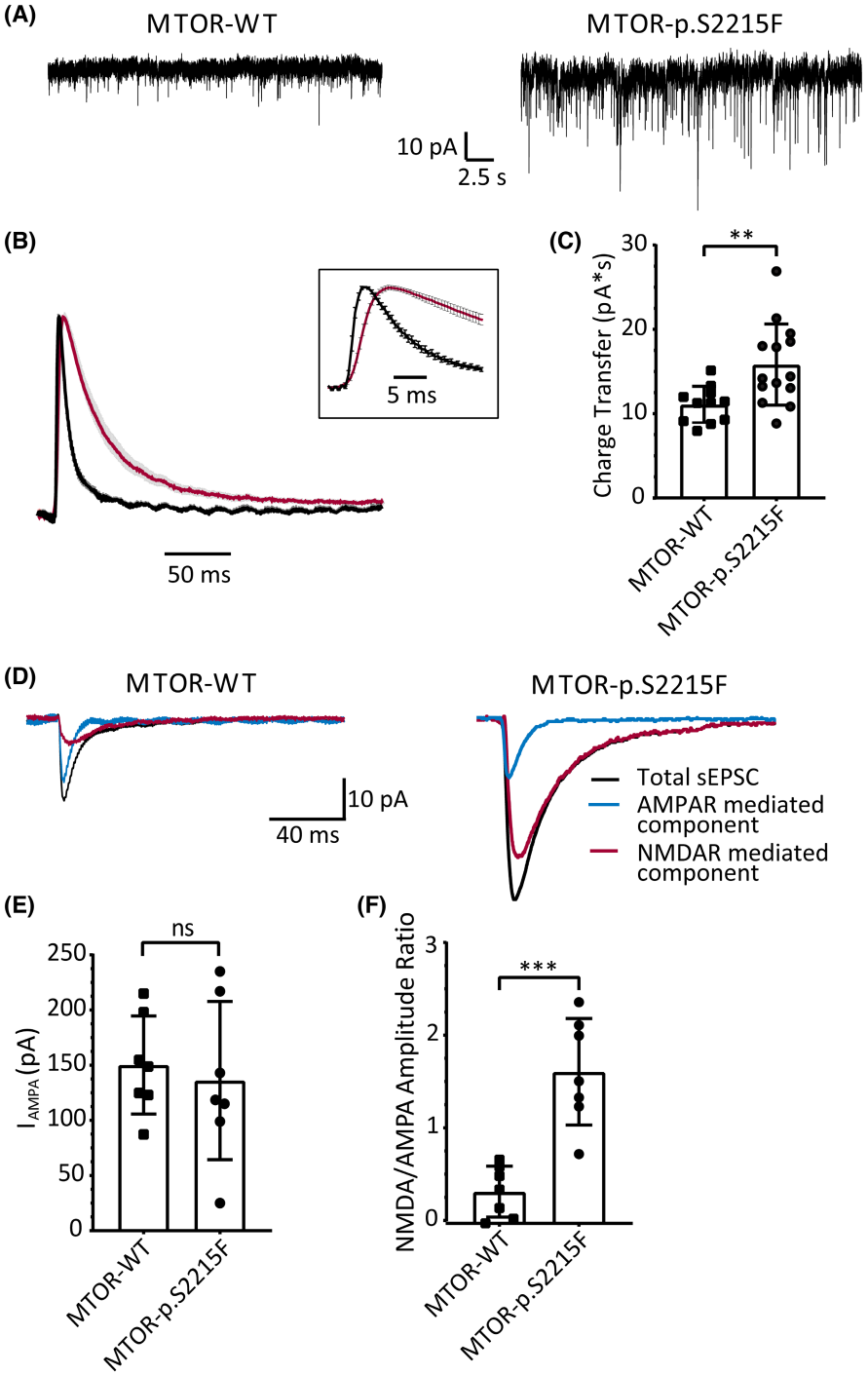

FIGURE 2 Spontaneous excitatory postsynaptic currents (sEPSCs) and N-methyl-D-aspartate (NMDA) to α-amino-3-hydroxy-5-methyl-4-isoxazolepropionic acid (AMPA) amplitude ratio in electroporated neurons. (A) Representative traces of sEPSCs in spiny stellate neurons expressing mechanistic target of rapamycin–wild type (MTOR-WT; left) and mutant MTOR-p.S2215F (right) recorded in Mg^{2+}-free artificial cerebrospinal fluid (ACSF) at −75 mV. (B) Averaged sEPSCs normalized to the peak for the WT (black) and the mutant (red) neurons. Note slower current decay and rise times (inset) for mutant neurons, indicating increased contribution of NMDA receptor (NMDAR)-mediated component on sEPSC amplitude. Values are given as mean ± SEM. (C) Total charge transfer through the sEPSCs normalized to the peak and calculated as an area under the composite sEPSC curve within 200 ms. MTOR-WT neurons, $n = 11$; mutant MTOR-p.S2215F neurons, $n = 14$. $^{**}p < .01$; Mann–Whitney test, two-tailed. (D) Representative traces of averaged sEPSCs recorded in MTOR-WT (left) and p.S2215F-MTOR (right) spiny stellate neurons in the following: black curve, drug-free (no drug) condition, representing total component of sEPSC; blue curve, after adding NMDAR blocker APV (50 μmol·L^{-1}), representing AMPA receptor (AMPAR)-mediated component of sEPSC; and red curve, after substraction of the AMPAR-mediated component from total sEPSC, representing NMDAR-mediated component of the sEPSC. Note the increased amplitude of the NMDAR-mediated component in the mutant MTOR-p.S2215F neurons, whereas the AMPAR-mediated component remains as in MTOR-WT neurons. (E) Summary data for AMPA component amplitude (I_{AMPA}) in MTOR-WT ($n = 7$) and MTOR-p.S2215F ($n = 7$) neurons. (F) Summary data for NMDA/AMPA amplitude ratios in MTOR- WT ($n = 7$) and in mutant MTOR-p.S2215F ($n = 7$) neurons. $^{***}p < .001$; ns, not significant; Mann–Whitney test, two-tailed.

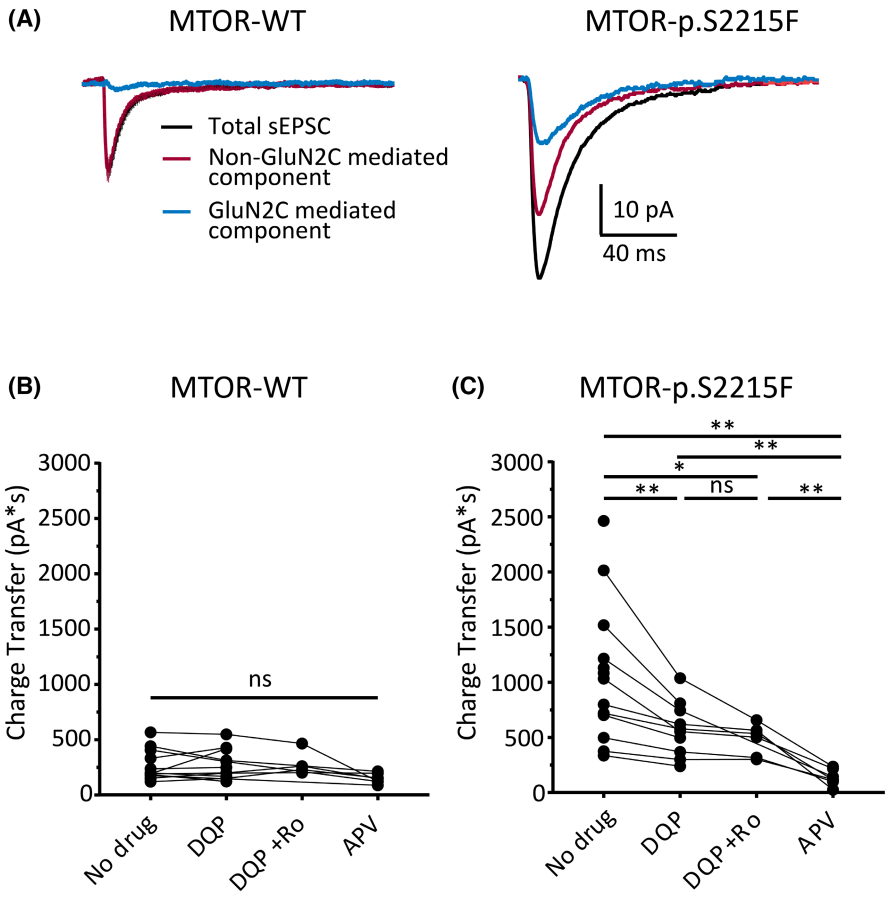

FIGURE 3 Functional upregulation of GluN2C-containing N-methyl-D-aspartate receptors (NMDARs) in mechanistic target of rapamycin (MTOR) p.S2215F electroporated neurons. (A) Representative traces of averaged spontaneous excitatory postsynaptic currents (sEPSCs) recorded in MTOR–wild-type (WT) (left) and MTOR-p.S2215F (right) spiny stellate neurons in the following: black curve, drug-free (no drug) condition, representing total component of sEPSC; red curve, after adding GluN2C-mediated NMDAR blocker DQP 1105 (10 μmol·L^{-1}), representing the non-GluN2C-mediated component of sEPSC; and blue curve, after subtraction of the non-GluN2C-mediated component from total sEPSC, hence representing GluN2C-mediated component of sEPSC. (B, C) Charge transfers were calculated in (B) MTOR-WT neurons and in (C) mutant MTOR-p.S2215F neurons, as areas between peak and 200 ms after the peak of the total sEPSC with the following: no drug, GluN2C blocker DQP 1105 (DQP; 10 μmol·L^{-1}), DQP 1105 (DQP; 10 μmol·L^{-1}) + GluN2B blocker Ro25-6981 (DQP+Ro; 1 μmol·L^{-1}), and total NMDAR blocker APV (50 μmol·L^{-1}). $^{*}p < .05$, $^{**}p < .01$; ns, not significant; mixed effect analysis with multiple comparison test.

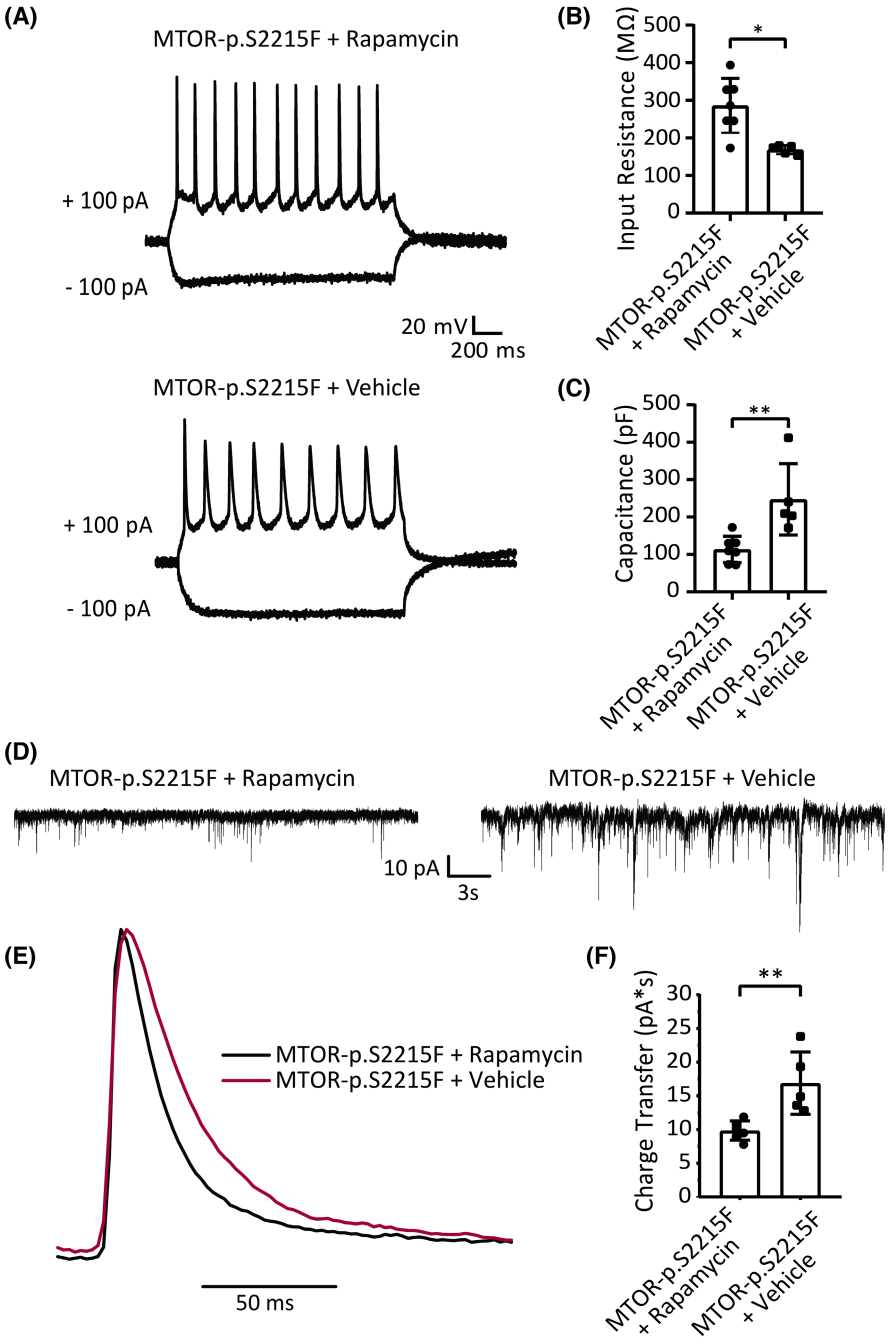

FIGURE 4 Rapamycin restores intrinsic properties and decreases the charge transfer of normalized spontaneous excitatory postsynaptic currents (sEPSCs) in mechanistic target of rapamycin (MTOR)–p.S2215F neurons. (A) Example traces of action potential firing patterns of spiny stellate neurons expressing MTOR-p.S2215F from pups treated with rapamycin (top) or vehicle (bottom), all recorded in current-clamp mode upon depolarizing and hyperpolarizing current injections. (B) Neuronal input resistance and (C) capacitance values in MTOR-p.S2215F + rapamycin ($n = 7$ neurons from four pups) and MTOR-p.S2215F + vehicle ($n = 5$ neurons from three pups) conditions. (D) Representative traces of sEPSCs from rapamycin (left) or vehicle (right) treated neurons expressing MTOR-p.S2215F, recorded in Mg^{2+}-free artificial cerebrospinal fluid at −75 mV. (E) Averaged sEPSCs normalized to the peak for the rapamycin (black) and vehicle (red) neurons. Note a slower current decay for neurons from rapamycin-treated pups, indicating increased contribution of N-methyl-D-aspartate receptor-mediated component on sEPSC amplitude. (F) Total charge transfer through the sEPSCs normalized to the peak and calculated as an area under the averaged sEPSC curve within 200 ms. MTOR-p.S2215F + rapamycine, $n = 6$ neurons from four pups; MTOR-p.S2215F + vehicle, $n = 5$ neurons from three pups. *$p < .05$, **$p < .01$; Mann–Whitney test, two-tailed.

P14–P16. A significant increase of spontaneous spiking activity frequency was observed in MTOR-p.S2215F slices (MTOR-p.S2215F: .8480 ± .5872 Hz; MTOR-WT: .3795 ± .5030 Hz; $p = .0434$; Figure 5A,B, Table S8). Importantly, this increased spiking activity was significantly inhibited when slices were acutely treated with

DQP 1105 in MTOR-p.S2215F condition, compared with the untreated condition; no additional effect was observed upon complete block of NMDARs with APV (no drug vs. DQP: $p = .0417$; no drug vs. APV: $p = .7907$; Figure 5C,D, Table S8), thus indicating that increased network activity in the local area containing a mosaic of *MTOR* mutant cells was mostly dependent on GluN2C-mediated NMDARs. In line with their favorable impact on NMDAR-mediated currents in mutant neurons, prior injections of rapamycin to the pups in vivo during seven consecutive days prevented against increased spiking activity in MTOR-p.S2215F slices (MTOR-p.S2215F, untreated: $1.901 \pm .9979$ Hz; MTOR-p.S2215F + rapamycin: $.5902 \pm .3601$ Hz; $p = .0337$; Figure 5E–G, Table S8).

We then decided to examine whether the GluN2C-dependent increased spontaneous spiking activity would be restricted to a critical time window, as reported in $Tsc^{+/-}$ mice.[14] Extracellular slice recordings done at P9 did not reveal any significant increase in spiking activity in the electroporated area in the mutant condition (Figure 6A,B); however, this spiking activity was driven by GluN2C-containing NMDARs, as shown by the significant impact of DQP 1105 on the frequency of spiking (Figure 6C, Table S9). Consistently, sEPSCs of MTOR-p.S2215F electroporated neurons at P9 showed a strong DQP 1105-sensitive component with a deactivation kinetic consistent with GluN2C-containing NMDAR-mediated currents (Figure S9). As at P9, at P20–P21 spontaneous spiking activity of slices from mTOR-p.S2215F electroporated animals, even though not increased compared with MTOR-WT slices (Figure 6D,E), was qualitatively modified, as it showed sensitivity to DQP 1105, whereas activity in MTOR-WT slices was not modified by DQP 1105 (Figure 6F, Table S9).

4 | DISCUSSION

Genetic defects leading to excessive activation of the mTOR pathway represent a well-established and important cause of various types of epileptic disorders, notably in the context of brain malformations.[2,3,23,24] However, the relationship with the underlying hyperexcitability remains to be clarified.[5,12] In the recent years, the involvement of somatic mTOR variants in FCD type II has been increasingly recognized.[25] We previously reported that the mosaic expression of a somatic, recurrent p.S2215F MTOR variant in neurons of the rat neocortex was associated with neuronal dyslamination and dysmorphia, two key hallmarks of FCD type II, and with increased S6 phosphorylation taken as a readout of mTORC1 overactivation.[15] In this model, we now show that SSNs expressing the mutant MTOR protein displayed intrinsic abnormalities and an excessive activation of NMDAR-mediated component of total sEPSCs not observed in MTOR-WT neurons, and sustained by GluN2C-containing NMDARs. Such an aberrant activity resulted in increased spontaneous spiking activity, revealing excessive local network activity that was restricted to a critical developmental time window. Slow decay kinetics of NMDAR GluN2C-mediated currents, leading to an increased synaptic integration, would facilitate neuronal network synchronicity. Hence, the GluN2C-dependent hyperexcitability previously reported in TSC[14] is now expanded to another type of mTORopathy and to another genetic context, namely FCD type II caused by a somatic, gain-of-function *MTOR* variant.

4.1 | From cell-autonomous GluN2C-related anomalies to hyperexcitability

Studies in different models of mTORopathies have pointed to nearly as many possible mechanisms of increased neuronal and network activities.[5] In our model, no change was detected in nonelectroporated neurons adjacent to the neurons expressing mutant MTOR. This is in line with other mosaic models of mTOR-related brain disorders, where cell-autonomous mechanisms were also reported.[26–28] As our analyses focused on the electroporated and their neighboring nonelectroporated SSNs, non-cell-autonomous effects on other cell types, such as pyramidal neurons, interneurons, or even non-neuronal cells, cannot be excluded; non-cell-autonomous changes, such as altered connectivity of distal neurons[29] or decreased density of interneurons,[30] were reported in other models of brain cortical malformations, including mTOR-related ones.[27,31,32] In a similar model of FCD, it was even shown that, compared to MTOR-WT neurons, neighboring cells were more excitable and sustained local epileptogenesis via adenosine release, whereas the mutant cells expressing MTOR-p.L2427P were less excitable.[31] Several nonexclusive reasons might account for this discrepancy, including the following: the possible different impacts that the p.S2215P and p.L2427P MTOR variants might have; the focus made only on SSNs with canonical firing patterns in the present study; the different conditions of current-clamp recordings; and the different time periods for whole-cell recordings (P14–P16 here vs. from 3 to 6 weeks of age[31]). Also, we do not exclude the participation of more distant cells or even of normotopic cortex (as in subcortical band heterotopia[33]) in FCD-related hyperexcitability; for instance, the increased bursting activity recorded in SSNs might well propagate to upper cortical layers, as previously shown in $Tsc^{+/-}$ mice.[14] In FCD tissues from patients and in animal models, the

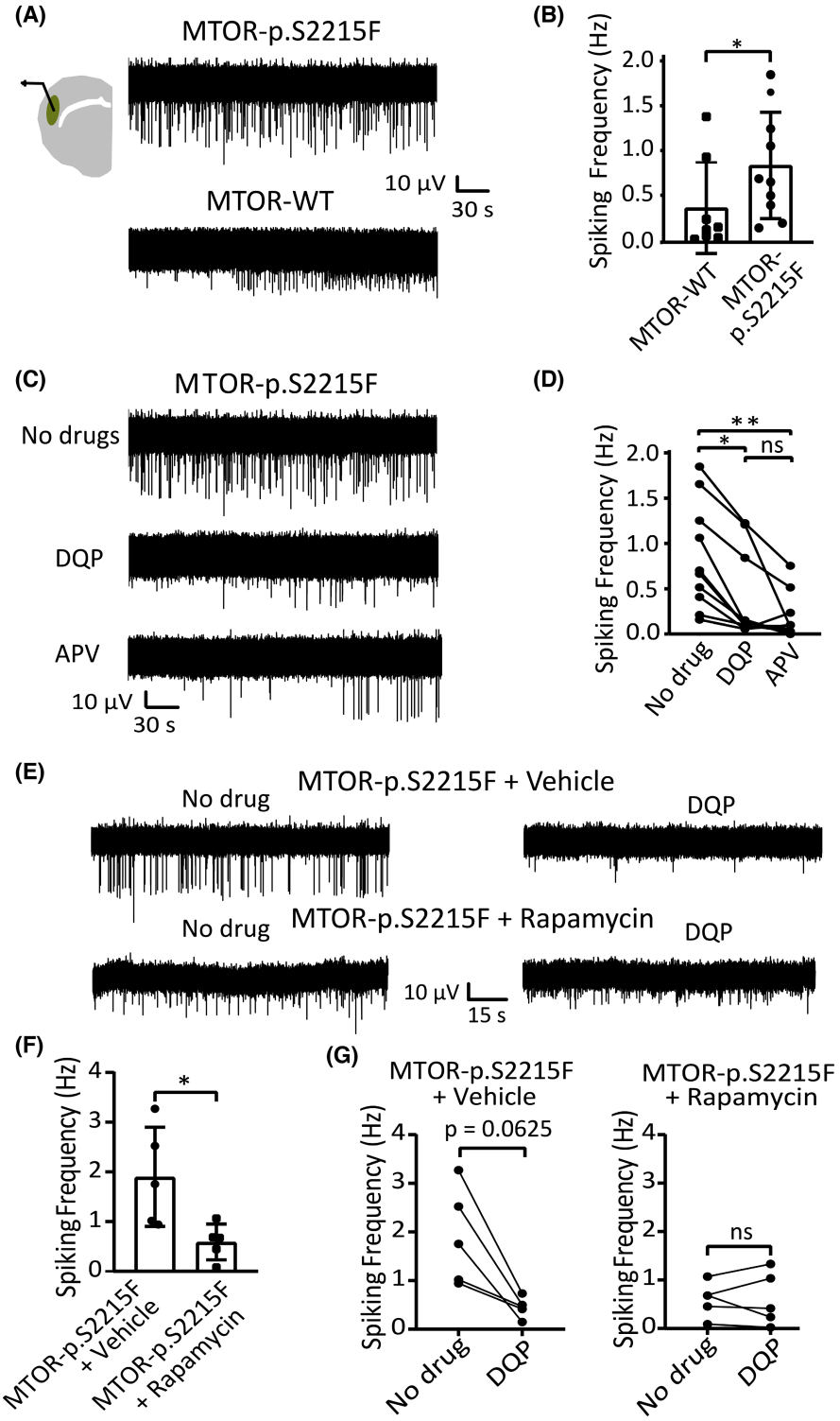

altered expression of $GABA_A$ receptors,[34] the increased expression of Kv1.1 potassium channels,[35] and the ectopic expression of HCN4-mediated Ih currents in mutant neurons[26] have been proposed. When different genetic models of focal mTORopathies were compared, both shared and divergent electrophysiological properties of the mutant neurons were found[36]; of note, the brain area (medial prefrontal cortex), the neuronal type (pyramidal neurons), and the developmental time point of the recordings (P28–P43) were all different from those studied here.

Our data point to a cell-autonomous role of overexpressed GluN2C-mediated NMDAR currents in SSNs. SSNs are considered to be the main acceptors of thalamic sensory inputs in the somatosensory cortex. They are excitatory cells that are highly interconnected within layer 4 and also have outputs in all cortical layers

FIGURE 5 Increased spiking activity in slices from mechanistic target of rapamycin (MTOR)–p.S2215F electroporated animals. (A) Representative traces of spontaneous activity recorded from green fluorescent electroporated areas in Mg^{2+}-containing artificial cerebrospinal fluid (ACSF) medium from (top trace) a mutant MTOR-p.S2215F slice and (bottom trace) an MTOR–wild-type (WT) slice. (B) Summary data for spiking frequency. MTOR-WT, $n = 8$ slices from seven pups; MTOR-p.S2215F, $n = 10$ slices from nine pups. $^*p < .05$; Mann–Whitney test, two-tailed. (C) Representative traces of spontaneous activity recorded in mutant MTOR-p.S2215F slices ($n = 10$ from nine pups) obtained in Mg^{2+}-containing ACSF with the following: (top) no drug, (middle) GluN2C blocker DQP 1105 (DQP, 10 μmol·L^{-1}), and (bottom) total N-methyl-D-aspartate receptor blocker APV (50 μmol·L^{-1}). (D) Summary data for spiking frequency. $^*p < .05$, $^{**}p < .01$; ns, not significant; Friedman test with Dunn multiple comparison test. (E) Representative traces of spontaneous activity recorded from the electroporated areas in Mg^{2+}-containing ACSF medium from the following: (top trace) a slice from a vehicle-treated, mutant MTOR-p.S2215F pup; and (bottom trace) a slice from a rapamycin-treated, mutant MTOR-p.S2215F pup without (no drug, left) or with DQP 1105 (DQP; 10 μmol·L^{-1}, right). (F) Summary data for spiking frequency; $n = 5$ slices from two pups in each condition. $^*p < .05$; Mann–Whitney test, two-tailed. (G) Summary data for spiking frequency without or with DQP 1105 for MTOR-p.S2215F + vehicle (left, $n = 5$ slices from two pups) and MTOR-p.S2215F + rapamycin (right, $n = 5$ slices from two pups). Note the statistical trend toward significant effect of DQP 1105 in the MTOR-p.S2215F + vehicle condition, as expected. Wilcoxon test, two-tailed.

in their own barrel and in adjacent ones. Considering the connectivity of SSNs and the specific properties of GluN2C-gated NMDAR currents, the overexpression of GluN2C-containing NMDAR currents in SSNs is very likely responsible for an increased probability of synchronizing neuronal activities. It is noteworthy that increased GluN2C-mediated NMDAR currents were also recorded in SSNs in *Tsc*$^{+/-}$ mice.[14] Of note, also, GluN2D-containing NMDARs would be sensitive to DQP 1105 and to other currently used GluN2C/D inhibitors[14,37,38]; however, the participation of GluN2D-NMDARs was excluded, as the decay kinetics of the component inhibited by DQP 1105 corresponded to GluN2C and not GluN2D contribution.[39]

4.2 | From mTORopathies to hyperexcitability: GluN2C-mediated neuronal NMDAR currents as a unifying mechanism

We had reported on the pathogenic role of GluN2C-mediated NMDARs in hyperexcitability of a TSC mouse model and of resected tissues from TSC patients.[14] Overexpression of *GRIN2C*, which encodes the GluN2C subunit, and GluN2C-dependent hyperexcitability, had already been detected in FCD tissues, albeit of undetermined genetic status.[14,34] We now demonstrate that GluN2C drives local hyperexcitability in the context of an MTOR pathogenic variant that is recurrently detected in FCD type II patients. As mTOR variants represent the majority of known somatic genetic causes of FCD type II, the GluN2C-related pathomechanism might well be shared in common by most type II FCDs. Treatment of the pups with rapamycin prior to the recordings prevented hyperactive NMDARs, GluN2C functional upregulation, and increased spontaneous spiking activity. This confirms that the p.S2215F variant does not impact on MTOR sensitivity to rapamycin.[40] MTOR is a member of both the mTORC1 and the mTORC2 complexes, and it was shown that rapamycin exerts its inhibitory effect on mTOR activity by targeting the MTOR protein in the mTORC1 but not in the mTORC2 complex.[41] Hence, our data indicate an important contribution of the mTORC1 pathway to pathogenesis in our model. Moreover, our data point to postsynaptic upregulation of NMDAR-mediated currents, which is consistent with previous findings showing that mTORC1 acted on glutamatergic synaptic transmission via a postsynaptic mechanism whereas mTORC2 affected presynaptic parameters.[42] Nonetheless, our data do not exclude the participation of mTORC1-independent pathological processes. For instance, it was shown that inhibition of mTORC2 reduced the neurobehavioral abnormalities of *Pten*-deficient mice[43] and, even more interestingly, of adult mice harboring the p.S2215F MTOR variant in a similar mosaic configuration as in the present study,[22] suggesting that both mTORC1- and mTORC2-related mechanisms would be operating, possibly at different developmental time points, in FCD caused by the p.S2215F MTOR variant.

As mTORC1 upregulation ultimately converges on dysregulated phosphorylation of shared downstream products, the GluN2C-mediated hyperexcitability might expand to an even broader spectrum of mTORC1-related disorders than TSC and FCD type II. Although this obviously warrants expanded confirmation in the corresponding models of mTORopathies, this would make it even more crucial to identify how mTOR hyperactivation leads to increased GluN2C-mediated NMDAR currents. Although we and others have previously demonstrated increased expression of the corresponding *GRIN2C* gene in human resected tissues and in mice,[14,34] what transcription and other factors would sustain *GRIN2C* dysregulation should be questioned in the future. Posttranscriptional effects of mTOR dysregulation on the expression of GluN2C-mediated currents, such as increased mTOR-dependent protein

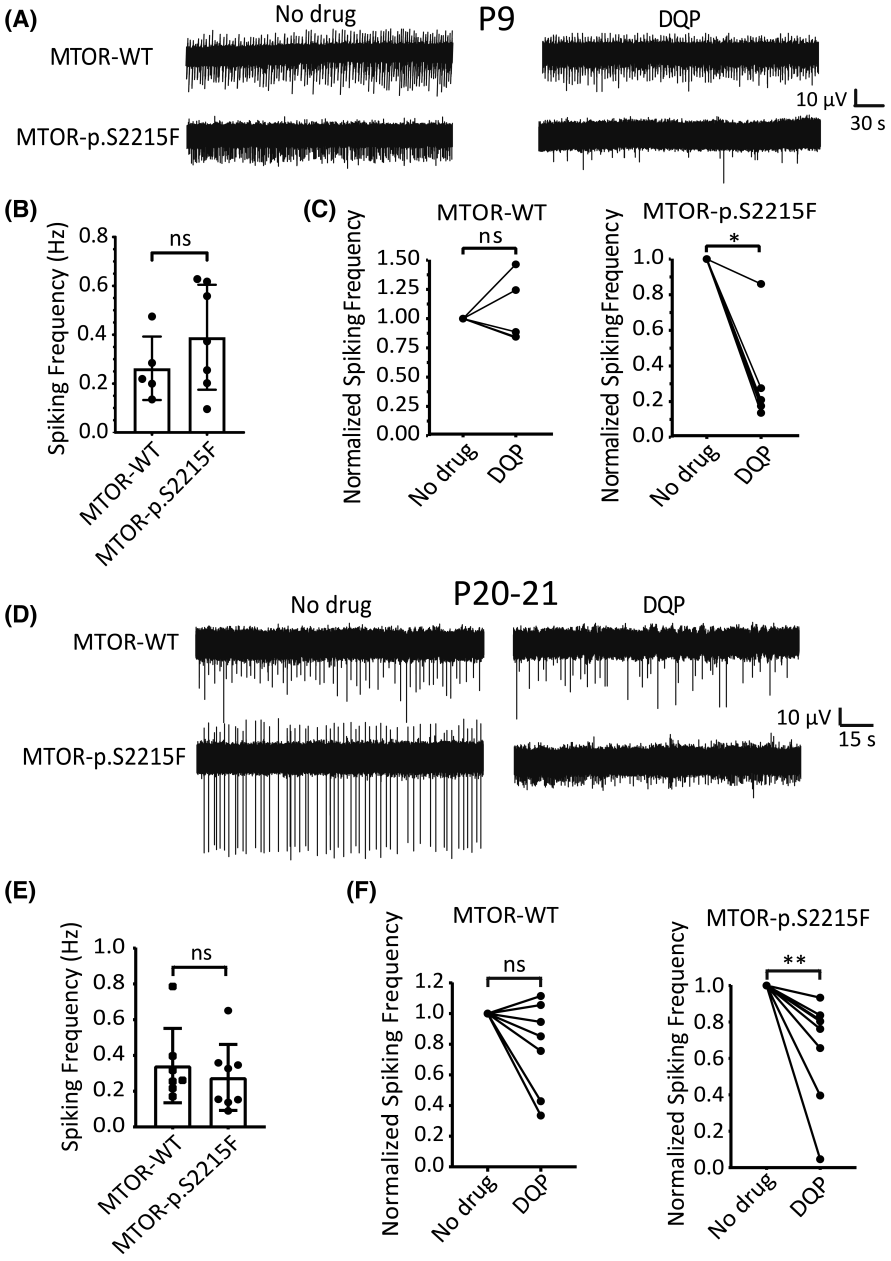

FIGURE 6 Developmental evolution of GluN2C-dependent increased spiking activity. (A) Representative traces of spontaneous activity recorded from electroporated areas in Mg^{2+}-containing artificial cerebrospinal fluid (ACSF) medium from (top trace) a mechanistic target of rapamycin–wild type (MTOR-WT) slice and (bottom trace) an MTOR-p.S2215F slice from P9 pups, without (no drug, left) or with DQP 1105 (DQP; 10 µmol·L^{-1}, right). (B) Summary data for spiking frequency. MTOR-WT, $n = 5$ slices from four pups; MTOR-p.S2215F, $n = 7$ from six pups. ns, not significant; Mann–Whitney test, two-tailed. (C) Summary data for spiking frequency without or with DQP 1105 for MTOR-WT (left) and MTOR-p.S2215F (right). Data shown are values normalized to the no-drug condition. *$p < .05$; Wilcoxon test, two-tailed. (D) Representative traces of spontaneous activity recorded from electroporated areas in Mg^{2+}-containing ACSF medium from (top trace) an MTOR-WT slice and (bottom trace) an MTOR-p.S2215F slice from P20–P21 pups without (No drug, left) or with DQP 1105 (10 µmol·L^{-1}, right). (E) Summary data for spiking frequency. MTOR-WT, $n = 7$ slices from four pups; MTOR-p.S2215F, $n = 8$ slices from five pups. Mann–Whitney test, two-tailed. (F) Summary data for spiking frequency without or with DQP 1105 for MTOR-WT (left) and MTOR-p.S2215F (right). Data shown are values normalized to the no-drug condition. **$p < .01$; Wilcoxon test, two-tailed.

translation or membrane trafficking, may be involved as well. Interestingly, the SSNs that had been electroporated in utero to express the WT isoform of MTOR did not show any quantitative or qualitative anomaly in NMDAR-mediated currents compared with the GFP-alone condition. GluN2C-mediated currents have been detected by single-channel recordings in SSNs of the somatosensory cortex in naive pups[44]; hence, mTOR

upregulation caused by MTOR-p.S2215F variant would be needed to trigger overexpression of GluN2C-mediated currents detectable by whole-cell recordings. This is in line with the lack of dyslamination and of neuronal dysmorphism observed here upon expression of WT MTOR, and with previous findings showing that overexpression of WT MTOR per se did not influence neuronal migration and morphology.[15,31,45,46]

4.3 | Critical time window for GluN2C-related pathomechanisms of mTORopathies?

As for epileptic activity in *Tsc1*$^{+/-}$ mice,[14] local hyperexcitability recorded at P14–P16 in neocortical slices looked transient, as it was detected neither at earlier (P9) nor at later (P20–P21) stages. Hence, GluN2C-mediated local hyperexcitability would follow the same developmental pattern in TSC and in FCD type II, being restricted to a similar critical developmental period. Interestingly, even though GluN2C-mediated component was upregulated and contributed to NMDAR-mediated currents in SSNs at P9, this was not sufficient to induce local hyperexcitability at that early stage. Also, compensatory mechanisms driven by developmental changes in the relative expression patterns of other NMDARs subunits, with GluN2A becoming predominant over GluN2B with age[39] and conferring faster kinetics to NMDARs, might explain why local hyperexcitability was no longer detected at the end of the third week of life. Our data also suggested that, in contrast with *Tsc*$^{+/-}$ mice, such a critical period of local hyperexcitability would not coincide with, but rather would precede the emergence of epileptic activity in our rat FCD model. In the mutant condition studied here, local hyperexcitability in the electroporated area in the second week of life was not associated with overt spontaneous epileptic seizure at the same age. Not all rodent models based on in utero electroporations and displaying neocortical dyslamination show overt seizures,[47,48] and this includes models of mTORopathies.[49,50] The mosaic characteristic of our model based on in utero electroporation, as compared with the constitutional Tsc$^{+/-}$ mouse model,[14] should be considered. Furthermore, the p.S2215F variant coexisted in one patient with another somatic variant in RPS6, a downstream protein of the mTOR pathway; this may suggest that additional events are needed for epilepsy to manifest clinically in the context of the somatic p.S2215F variant. However, the p.S2215F variant has been recurrently detected in many FCD type II patients[16–18] and hence is likely to be pathogenic on its own, as also shown in the present study. Epileptic discharges and frequent spike–waves were detected at P60–P70 in the mutant rats, long after the critical time period for GluN2C-mediated hyperexcitability. These data indicate that epileptic activity in older rats would emerge after a previous and time-restricted local hyperexcitability in the brain area displaying MTOR mutant neurons. The likely multiple (e.g., neuroinflammation, impaired connectivity) and complicated proepileptogenic processes that would follow the GluN2C-dependent, time-restricted excessive local network activity remain to be clarified.

Our data make the GluN2C-containing NMDAR a possible target in FCD type II caused by somatic variants of the mTOR pathway, as previously suggested for autosomal dominant TSC.[14,51] The importance of GluN2C in FCD pathogenesis might even expand beyond the spectrum of mTORopathies, as recently suggested by the detection of a somatic *GRIN2C* variant in a patient with FCD type I.[52] Our results indicate a critical time window for GluN2C-mediated pathomechanisms and for related rescue strategies. Although efforts toward the development of novel GluN2C-selective inhibitors are ongoing,[51,53] possible off-target effects of GluN2C inhibition should be considered. Not being detectable at birth, mouse GluN2C expression is enriched in the second postnatal week in the cerebellum, the thalamic reticular nucleus, and the olfactory bulb.[39,54] Systemic administration of GluN2C inhibitors would likely impact on NMDARs expressed in such distant brain areas, and GluN2C influences cortical excitation/inhibition balance and neuronal oscillations.[55] Administration at the lesion location would likely prevent such broad side effects; however, GluN2C-mediated currents are also detectable in SSNs in physiological conditions, and can be expressed in nonneuronal cells.[54,56] Despite these limitations, our data suggest that early, focal inhibition of GluN2C-mediated currents during a critical time period should be considered in FCD type II. Early interventions against mTOR-related dysregulations are also being considered to prevent against the progression to severe epilepsy in TSC.[11]

5 | CONCLUSIONS

Slow decay kinetics of GluN2C-mediated NMDAR currents, by leading to increased synaptic integration, facilitate neuronal network synchronicity. We show that GluN2C-containing NMDARs drive time-restricted local hyperexcitability in the context of an MTOR somatic variant that was recurrently detected in FCD type II patients. As somatic variants of the mTOR pathway represent an important cause of FCD type II, the GluN2C-related mechanism of focal mTORopathy might well be shared in common by most type II FCDs, and beyond in the context of other mTORopathies.

AUTHOR CONTRIBUTIONS

Louison Pineau performed most experiments, did most data analysis of recordings with Nail Burnashev, and wrote the article with Pierre Szepetowski and Nail Burnashev. Emmanuelle Buhler performed the in utero intracerebroventricular electroporations and the EEG recordings. Sarah Tarhini participated in immunohistochemical (IHC) experiments and in extracellular electrophysiological recordings and analyses. Sylvian Bauer participated in follow-up of the study and in IHC experiments. Valérie Crepel analyzed EEG traces with Louison Pineau. Françoise Watrin, Carlos Cardoso, and Alfonso Represa participated in the design and follow-up of the study. Pierre Szepetowski and Nail Burnashev codecided on the overall strategy, codirected the follow-up of experiments, and wrote the article. All authors contributed the final version of the article.

ACKNOWLEDGMENTS

We thank E. Bouilloc, P. Moudery, and S. Corby for their help at INMED (Mediterranean Institute of Neurobiology) animal core facilities, A. Montheil and E. Pallesi-Pocachard at INMED Molecular and Cell Biology platform, and F. Michel at INMED InMagic platform. We also thank L. Aniksztejn for his advice on electrophysiological recordings. L.P. has been a recipient of a Ministry of Research Aix-Marseille University Doctoral School (ED62) PhD fellowship. S.T. is a recipient of an Aix-Marseille University/A*MIDEX /CMA CGM PhD fellowship. This work was supported by INSERM (Institut National de la Santé et de la Recherche Médicale) and by the European Union Seventh Framework Program FP7/2007-2013 under the project DESIRE (grant agreement No. 602531).

CONFLICT OF INTEREST STATEMENT

V.C. and A.R. filed a patent by Inserm Transfert for "Method and Pharmaceutical Composition for Use in the Treatment of Focal Cortical Dysplasia" (2023), which is not associated with the present study. V.C. has received funding support from uniQure, which is not associated with the present study. The remaining authors have no conflicts of interest to disclose.

ETHICS STATEMENT

Animal experimentations were performed according to French legislation and in compliance with European Communities Council Directives (2010/63/UE). This study was approved under the French Department of Agriculture and the local veterinary authorities by the Animal Experimentation Ethics Committee No. 14 under license APAFIS#23362-2019121712305437-v4. We confirm that we have read the Journal's position on issues involved in ethical publication and affirm that this report is consistent with those guidelines.

ORCID

Pierre Szepetowski https://orcid.org/0000-0003-2060-8390
Nail Burnashev https://orcid.org/0000-0002-0478-3810

REFERENCES

1. Szwed A, Kim E, Jacinto E. Regulation and metabolic functions of mTORC1 and mTORC2. Physiol Rev. 2021;101:1371–426.
2. Baulac S. Chapter 3—mTOR signaling pathway genes in focal epilepsies. In: Rossignol E, Carmant L, Lacaille J-C, editors. Progress in brain research. Volume 226. Amsterdam: Elsevier; 2016. p. 61–79.
3. Crino PB. mTOR signaling in epilepsy: insights from malformations of cortical development. Cold Spring Harb Perspect Med. 2015;5:a022442.
4. Marsan E, Baulac S. Review: mechanistic target of rapamycin (mTOR) pathway, focal cortical dysplasia and epilepsy. Neuropathol Appl Neurobiol. 2018;44:6–17.
5. Nguyen LH, Bordey A. Convergent and divergent mechanisms of epileptogenesis in mTORopathies. Front Neuroanat. 2021;15:664695.
6. Blumcke I, Cendes F, Miyata H, Thom M, Aronica E, Najm I. Toward a refined genotype–phenotype classification scheme for the international consensus classification of focal cortical dysplasia. Brain Pathol. 2021;31:e12956.
7. Mühlebner A, Bongaarts A, Sarnat HB, Scholl T, Aronica E. New insights into a spectrum of developmental malformations related to mTOR dysregulations: challenges and perspectives. J Anat. 2019;235:521–42.
8. Baldassari S, Ribierre T, Marsan E, Adle-Biassette H, Ferrand-Sorbets S, Bulteau C, et al. Dissecting the genetic basis of focal cortical dysplasia: a large cohort study. Acta Neuropathol. 2019;138:885–900.
9. Becker AJ, Beck H. New developments in understanding focal cortical malformations. Curr Opin Neurol. 2018;31:151–5.
10. Blumcke I, Spreafico R, Haaker G, Coras R, Kobow K, Bien CG, et al. Histopathological findings in brain tissue obtained during epilepsy surgery. N Engl J Med. 2017;377:1648–56.
11. Aronica E, Specchio N, Luinenburg MJ, Curatolo P. Epileptogenesis in tuberous sclerosis complex-related developmental and epileptic encephalopathy. Brain. 2023;146:2694–710.
12. Represa A. Why malformations of cortical development cause epilepsy. Front Neurosci. 2019;13:250. https://doi.org/10.3389/fnins.2019.00250
13. Hansen KB, Yi F, Perszyk RE, Menniti FS, Traynelis SF. NMDA receptors in the central nervous system. Methods Mol Biol. 2017;1677:1–80.
14. Lozovaya N, Gataullina S, Tsintsadze T, Tsintsadze V, Pallesi-Pocachard E, Minlebaev M, et al. Selective suppression of excessive GluN2C expression rescues early epilepsy in a tuberous sclerosis murine model. Nat Commun. 2014;5:4563.
15. Pelorosso C, Watrin F, Conti V, Buhler E, Gelot A, Yang X, et al. Somatic double-hit in MTOR and RPS6 in hemimegalencephaly with intractable epilepsy. Hum Mol Genet. 2019;28:3755–65. https://doi.org/10.1093/hmg/ddz194

16. Mirzaa GM, Campbell CD, Solovieff N, Goold CP, Jansen LA, Menon S, et al. Wide spectrum of developmental brain disorders from megalencephaly to focal cortical dysplasia and pigmentary mosaicism caused by mutations of MTOR. JAMA Neurol. 2016;73:836–45.
17. Møller RS, Weckhuysen S, Chipaux M, Marsan E, Taly V, Bebin EM, et al. Germline and somatic mutations in the MTOR gene in focal cortical dysplasia and epilepsy. Neurol Genet. 2016;2:e118.
18. Nakashima M, Saitsu H, Takei N, Tohyama J, Kato M, Kitaura H, et al. Somatic mutations in the MTOR gene cause focal cortical dysplasia type IIb. Ann Neurol. 2015;78:375–86.
19. Scala F, Kobak D, Shan S, Bernaerts Y, Laturnus S, Cadwell CR, et al. Layer 4 of mouse neocortex differs in cell types and circuit organization between sensory areas. Nat Commun. 2019;10:4174.
20. Staiger JF, Flagmeyer I, Schubert D, Zilles K, Kötter R, Luhmann HJ. Functional diversity of layer IV spiny neurons in rat somatosensory cortex: quantitative morphology of electrophysiologically characterized and biocytin labeled cells. Cereb Cortex. 2004;14:690–701.
21. Sahu S, Buhler E, Vermoyal JC, Watrin F, Represa A, Manent JB. Spontaneous epileptiform activity in a rat model of bilateral subcortical band heterotopia. Epilepsia. 2019;60:337–48.
22. Okoh J, Mays J, Bacq A, Oses-Prieto JA, Tyanova S, Chen CJ, et al. Targeted suppression of mTORC2 reduces seizures across models of epilepsy. Nat Commun. 2023;14:7364.
23. Aronica E, Becker AJ, Spreafico R. Malformations of cortical development. Brain Pathol. 2012;22:380–401.
24. Blümcke I, Coras R, Busch RM, Morita-Sherman M, Lal D, Prayson R, et al. Toward a better definition of focal cortical dysplasia: an iterative histopathological and genetic agreement trial. Epilepsia. 2021;62:1416–28.
25. Blumcke I, Budday S, Poduri A, Lal D, Kobow K, Baulac S. Neocortical development and epilepsy: insights from focal cortical dysplasia and brain tumours. Lancet Neurol. 2021;20:943–55.
26. Hsieh LS, Wen JH, Claycomb K, Huang Y, Harrsch FA, Naegele JR, et al. Convulsive seizures from experimental focal cortical dysplasia occur independently of cell misplacement. Nat Commun. 2016;7:11753.
27. Park SM, Lim JS, Ramakrishina S, Kim SH, Kim WK, Lee J, et al. Brain somatic mutations in MTOR disrupt neuronal ciliogenesis leading to focal cortical dyslamination. Neuron. 2018;99:83–97.e7.
28. Wu X, Sosunov AA, Lado W, Teoh JJ, Ham A, Li H, et al. Synaptic hyperexcitability of cytomegalic pyramidal neurons contributes to epileptogenesis in tuberous sclerosis complex. Cell Rep. 2022;40:111085.
29. Proietti Onori M, Koene LMC, Schäfer CB, Nellist M, de Brito van Velze M, Gao Z, et al. RHEB/mTOR hyperactivity causes cortical malformations and epileptic seizures through increased axonal connectivity. PLoS Biol. 2021;19:e3001279.
30. Zhong S, Zhao Z, Xie W, Cai Y, Zhang Y, Ding J, et al. GABAergic interneuron and neurotransmission are mTOR-dependently disturbed in experimental focal cortical dysplasia. Mol Neurobiol. 2021;58:156–69.
31. Kim JK, Cho J, Kim SH, Kang HC, Kim DS, Kim VN, et al. Brain somatic mutations in MTOR reveal translational dysregulations underlying intractable focal epilepsy. J Clin Invest. 2019;129:4207–23.
32. Koh HY, Jang J, Ju SH, Kim R, Cho GB, Kim DS, et al. Non-cell autonomous Epileptogenesis in focal cortical dysplasia. Ann Neurol. 2021;90:285–99.
33. Petit LF, Jalabert M, Buhler E, Malvache A, Peret A, Chauvin Y, et al. Normotopic cortex is the major contributor to epilepsy in experimental double cortex. Ann Neurol. 2014;76:428–42.
34. Crino PB, Duhaime AC, Baltuch G, White R. Differential expression of glutamate and GABA-A receptor subunit mRNA in cortical dysplasia. Neurology. 2001;56:906–13.
35. Nguyen LH, Anderson AE. mTOR-dependent alterations of Kv1.1 subunit expression in the neuronal subset-specific Pten knockout mouse model of cortical dysplasia with epilepsy. Sci Rep. 2018;8:3568.
36. Nguyen LH, Xu Y, Nair M, Bordey A. The mTOR pathway genes mTOR, Rheb, Depdc5, Pten, and Tsc1 have convergent and divergent impacts on cortical neuron development and function. *bioRxiv* 2023 https://doi.org/10.1101/2023.08.11.553034
37. Acker TM, Yuan H, Hansen KB, Vance KM, Ogden KK, Jensen HS, et al. Mechanism for noncompetitive inhibition by novel GluN2C/D N-methyl-D-aspartate receptor subunit-selective modulators. Mol Pharmacol. 2011;80:782–95.
38. Wang JX, Irvine MW, Burnell ES, Sapkota K, Thatcher RJ, Li M, et al. Structural basis of subtype-selective competitive antagonism for GluN2C/2D-containing NMDA receptors. Nat Commun. 2020;11:423.
39. Monyer H, Burnashev N, Laurie DJ, Sakmann B, Seeburg PH. Developmental and regional expression in the rat brain and functional properties of four NMDA receptors. Neuron. 1994;12:529–40.
40. Xu J, Pham CG, Albanese SK, Dong Y, Oyama T, Lee CH, et al. Mechanistically distinct cancer-associated mTOR activation clusters predict sensitivity to rapamycin. J Clin Invest. 2016;126:3526–40.
41. Seto B. Rapamycin and mTOR: a serendipitous discovery and implications for breast cancer. Clin Transl Med. 2012;1:29.
42. McCabe MP, Cullen ER, Barrows CM, Shore AN, Tooke KI, Laprade KA, et al. Genetic inactivation of mTORC1 or mTORC2 in neurons reveals distinct functions in glutamatergic synaptic transmission. elife. 2020;9:e51440.
43. Chen C-J, Sgritta M, Mays J, Zhou H, Lucero R, Park J, et al. Therapeutic inhibition of mTORC2 rescues the behavioral and neurophysiological abnormalities associated with Pten-deficiency. Nat Med. 2019;25:1684–90.
44. Scheppach C. High- and low-conductance NMDA receptors are present in layer 4 spiny stellate and layer 2/3 pyramidal neurons of mouse barrel cortex. Physiol Rep. 2016;4:e13051.
45. Kassai H, Sugaya Y, Noda S, Nakao K, Maeda T, Kano M, et al. Selective activation of mTORC1 signaling recapitulates microcephaly, tuberous sclerosis, and neurodegenerative diseases. Cell Rep. 2014;7:1626–39.
46. Lim JS, Kim WI, Kang HC, Kim SH, Park AH, Park EK, et al. Brain somatic mutations in MTOR cause focal cortical dysplasia type II leading to intractable epilepsy. Nat Med. 2015;21:395–400.
47. Goz RU, Akgül G, LoTurco JJ. BRAFV600E expression in neural progenitors results in a hyperexcitable phenotype in neocortical pyramidal neurons. J Neurophysiol. 2020;123:2449–64.

48. Salmi M, Bruneau N, Cillario J, Lozovaya N, Massacrier A, Buhler E, et al. Tubacin prevents neuronal migration defects and epileptic activity caused by rat Srpx2 silencing in utero. Brain. 2013;136:2457–73.
49. Lin TV, Hsieh L, Kimura T, Malone TJ, Bordey A. Normalizing translation through 4E-BP prevents mTOR-driven cortical mislamination and ameliorates aberrant neuron integration. Proc Natl Acad Sci USA. 2016;113:11330–35.
50. Zhang L, Huang T, Teaw S, Bordey A. Hypervascularization in mTOR-dependent focal and global cortical malformations displays differential rapamycin-sensitivity. Epilepsia. 2019;60:1255–65.
51. Gataullina S, Galvani G, Touchet S, Nous C, Lemaire É, Laschet J, et al. GluN2C selective inhibition is a target to develop new antiepileptic compounds. Epilepsia. 2022;63:2911–24.
52. Chung C, Yang X, Bae T, Vong KI, Mittal S, Donkels C, et al. Comprehensive multi-omic profiling of somatic mutations in malformations of cortical development. Nat Genet. 2023;55:209–20.
53. D'Erasmo MP, Akins NS, Ma P, Jing Y, Swanger SA, Sharma SK, et al. Development of a dihydroquinoline-pyrazoline GluN2C/2D-selective negative allosteric modulator of the N-methyl-d-aspartate receptor. ACS Chem Neurosci. 2023;14:3059–76.
54. Ravikrishnan A, Gandhi PJ, Shelkar GP, Liu J, Pavuluri R, Dravid SM. Region-specific expression of NMDA receptor GluN2C subunit in parvalbumin-positive neurons and astrocytes: analysis of GluN2C expression using a novel reporter model. Neuroscience. 2018;380:49–62.
55. Gupta SC, Ravikrishnan A, Liu J, Mao Z, Pavuluri R, Hillman BG, et al. The NMDA receptor GluN2C subunit controls cortical excitatory-inhibitory balance, neuronal oscillations and cognitive function. Sci Rep. 2016;6:38321.
56. Alsaad HA, DeKorver NW, Mao Z, Dravid SM, Arikkath J, Monaghan DT. In the telencephalon, GluN2C NMDA receptor subunit mRNA is predominately expressed in glial cells and GluN2D mRNA in interneurons. Neurochem Res. 2019;44:61–77.

SUPPORTING INFORMATION

Additional supporting information can be found online in the Supporting Information section at the end of this article.

How to cite this article: Pineau L, Buhler E, Tarhini S, Bauer S, Crepel V, Watrin F, et al. Pathogenic *MTOR* somatic variant causing focal cortical dysplasia drives hyperexcitability via overactivation of neuronal GluN2C N-methyl-D-aspartate receptors. Epilepsia. 2024;65:2111–2126. https://doi.org/10.1111/epi.18000